Magnitude Least Squares Optimization for Parallel RF Excitation Design Demonstrated at 7 Tesla with 8 Channels

K. Setsompop[1], V. Alagappan[2], B. Gagoski[1], L. Wald[3], and E. Adalsteinsson[1]

[1]EECS, Massachusetts Institute of Technology, Cambridge, ma, United States, [2]A. A. Martinos Center for Biomedical Imaging, MGH, Charlestown, ma, United States, [3]A. A. Martinos Center for Biomedical Imaging, Department of Radiology, MGH, Charlestown, MA, United States

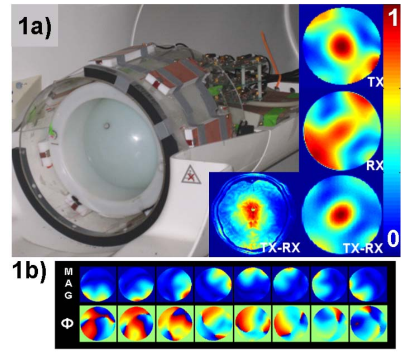

Introduction: Parallel RF excitations (pTx) are often designed as a least-squares (LS) optimized approximation to a target magnitude and phase profile. However, adherence to the target *phase* profile is usually not important as long as the excitation phase is slowly varying compared to the voxel dimension. Kerr et al. [1] proposed an approach for magnitude-least-squares (MLS) optimization of the target magnetization profile and demonstrate its benefit in reducing excitation error for a spiral excitation. In this work, we outline a different method for MLS optimization to improve both the magnitude profile and reduce the RF power while maintaining a smoothly and slowly varying phase profile. We validate the method with a slice selective spoke excitation for in-plane B_1^+ mitigation, and a 4-fold (R=4) accelerated 2D spiral excitation using an 8-channel transmit array on a 7T human MRI scanner. The method resulted in significant improvements over LS, especially for the spoke excitation where a 34% drop in root magnitude mean square error (RMMSE) and 49% drop in integrated RF power were observed.

Theory: We formulated pTx as in Grissom et al [2], where the RF is normally designed by solving, by LS: $b = \arg_b \min\{\|Ab - m\|_w^2 + \beta\|b\|_2^2\}$, with the optimization performed over the ROI implied by a weighting, w, and where $\beta\|b\|_2^2$ denotes a Tikhonov regularization term to manage integrated RF power. Here, MLS optimization is posed as: $b = \arg_b \min\{\|\,|Ab| - m\,\|_w^2 + \beta\|b\|_2^2\}$, and is used to improve the magnitude profile and reduce the RF power at the cost of a less uniform phase profile. We based our optimization on the local-variable exchange method proposed by Kassakian [3], but additionally impose a mild constraint on the spatial phase in the form of a smooth and slowly varying spatial phase profile to minimize intra-voxel dephasing. This mild phase constraint is achieved by smoothing the resulting phase profile at each iteration step with a Gaussian filter, thereby forcing the phase profile to evolve smoothly.

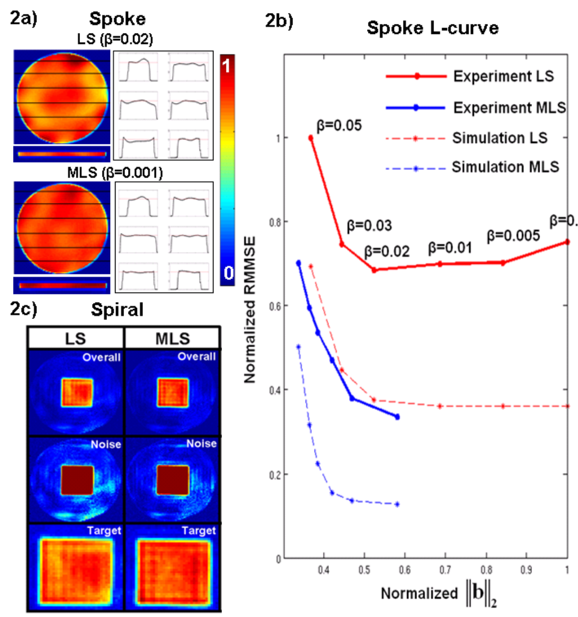

Methods: To compare the performance of the LS and MLS optimizations, a slice selective 4-spoke excitation (2.86ms duration) and a 4X accelerated 2D spiral excitations (3.51 ms) with a square target profile were designed and tested using an 8-channel TX-RX stripline coil array (fig.1), on a Siemens 7T Magnetom scanner equipped with an 8-channel pTx system. For a comprehensive comparison, in both types of excitations, we designed the RF pulses for a range of Tikhonov regularization values, β, so that the performance of the optimization could be compared over a range of "magnitude profile error vs. RF power" tradeoff points (L-curve). The metric used to quantify the deviation from the target profile is RMMSE, defined here as: $RMMSE = \sqrt{\|\,|Ab| - m\,\|_w^2}$. The RF power metric used is the RF voltage norm ($\|b\|_2$).

All measurements were performed in a 17-cm diameter doped water phantom with cylindrical loading ring used to mimic the human load. B_1^+ maps of the 8 transmit channels were obtained by first estimating the birdcage receive profile via transmitting and receiving with the birdcage mode at a set of voltage levels and using a Simplex algorithm in Matlab to fit the resulting intensities to the equation: $I(x,y) = RX(x,y) \times \frac{[1 - e^{-TR/T_1(x,y)}]\sin\theta(x,y)}{1 - e^{-TR/T_1(x,y)}\cos\theta(x,y)}$. Once the birdcage receive profile (RX) is obtained, the profile of each transmit channel can be estimated by obtaining a low-flip-angle image on each channel (TR=1s>>T1=0.165s) and dividing the image by the birdcage receive profile. This procedure yielded quantitative $B_1^+(x,y)$ maps in [G/V].

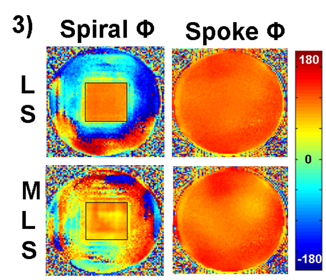

Results: Figure 1a (bottom right, marked TX-RX) illustrates the image using a birdcage phase relationship for transmit and receive in a human brain and for the water phantom. Each show a factor ~9 variation peak-to-valley in magnitude. Also shown are the measured TX and RX birdcage profiles. The transmit magnitude and phase profiles of each individual coil are shown in Fig. 1b. Figure 2a shows a comparison between the best (lowest RMMSE) 4-spoke excitation achieved using LS and MLS design. The MLS design reduced RMMSE by 51%. Figure 2b shows the plot of the normalized RMMSE vs. RF voltage amplitude. With MLS optimization, the average drop in RMMSE and integrated RF power over the experimental data points were 34% and 49%. Figure 2c shows the comparison between LS and MLS design for the square-target spiral based excitation at β = 1.5, where the MLS design resulted in a reduction in RMMSE of 15.62%. The images in row 2 & 3 are scaled to visualize the improved background noise suppression and better square target excitation resulting from the MLS design. The average drops in RMMSE and integrated RF power (over a comparable β range as in the spoke case) were 10% and 5.7%. Figure 3 shows the increases in spatial phase variation traded-off for lower RMMSE and RF power for both of the spoke and spiral excitations. In both cases the phase variation is small and smoothly varying, resulting in negligible intra-voxel dephasing.

Discussion and Conclusion: In this work we demonstrate the benefits of MLS optimization in pTx design using a water phantom with large B_1 profile variation, similar to that observed in human brain at 7T. Given the significant benefit achieved with the MLS optimization, particularly for the mitigation of the inhomogeneous B_1^+ profile through the use of the spoke trajectory excitation, we expect the MLS optimization to play an important role in parallel excitation design for human imaging at high field.

Support: NIH R01EB006847, R01EB007942, R01EB000790, and NCRR grant P41RR14075, Siemens Medical Solutions, R.J.Shillman Career Development Award, and the MIND Institute. **References:** **[1]** Kerr A. et al, ISMRM 2007: p.1693; **[2]** Grissom W. et al, MRM 56:620, 2006; **[3]** Kassakian PW., UCB PhD Thesis 2006;